Sigma J Eng Nat Sci, Vol. 44, No. 1, pp. 115–126, February, 2026

Sigma Journal of Engineering and Natural Sciences
Web page info: https://sigma.yildiz.edu.tr
DOI: 10.14744/sigma.2026.1972

Research Article

Study of improved quantum particle swarm optimization for modeling of wasted surgical mask

Subhojit CHATTARAJ[1,*], Sk Tanbir ISLAM[2], Pijush DUTTA[3], Mahuya DAS[4]

[1]Department of Civil Engineering, Greater Kolkata College of Engineering and Management, Kolkata, 743387, India
[2]Department of Mechanical Engineering, Greater Kolkata College of Engineering and Management, Kolkata, 743387, India
[3]Department of Computer Science Engineering, Greater Kolkata College of Engineering and Management, Kolkata, 743387, India
[4]Department of Chemistry, Bankura Zilla Saradamani Mahila Mahabivyapith Nutanchati, West Bengal, 722101, India

ARTICLE INFO

Article history
Received: 16 June 2024
Revised: 21 August 2024
Accepted: 13 January 2025

Keywords:
Artificial Neural Network (ANN); Improved Particle Swarm Optimization; Parametric Optimization; Plastic Board

ABSTRACT

The complexity of real-world optimization problems has been steadily driving computer science researchers to come up with new and efficient optimization techniques. Precise modeling of the plastic boards by use of experimental data, in which discarded surgical masks are used, is a major challenge to engineering professionals. In this article, a Modified Gaussian Quantum Particle Swarm Optimization (GQPSO) is proposed for the efficient and accurate estimation of manufacturing plastic board characteristics. The algorithm was initially tested using two benchmark functions, which included Elongation at fracture (EF) and Percentage of total elongation at maximum force (MF), using material compositions including those of polypropylene (PP), Maleic anhydride Grafted Polypropylenes (MA), Titanium dioxide (TiO2), and Tensile Strength (TS). Experiment findings and comparisons with other optimization techniques clearly show that this suggested method is successful in terms of final solution correctness, success rate, convergence speed, and stability. The suggested GQPSO optimization approach was then evaluated against the manufacturer's datasheet of the optimal outcome of both elongations at fracture and the percentage of total elongation at maximum force are 29.678%, 11.082%, 0.4412%, and 26.712, respectively for polypropylene (PP), Maleic anhydrite Grafted polypropylene (MA), Titanium dioxide (TiO2), and Tensile Strength (TS) during waste surgical mask design. The findings prove the efficiency of the Gaussian Quantum-behaved Particle swarm optimization (GQPSO) algorithm in different working conditions.

Cite this article as: Chattaraj S, Islam ST, Dutta P, Mahuya DASM. Study of improved quantum particle swarm optimization for modeling of wasted surgical mask. Sigma J Eng Nat Sci 2026;44(1):115–126.

***Corresponding author.**
*E-mail address: subhojitchattaraj@gmail.com

This paper was recommended for publication in revised form by Editor-in-Chief Ahmet Selim Dalkilic

INTRODUCTION

The daily applications of plastic polymers have a number of good effects in society, but the microplastic (MP) particles linked with the plastic era have health and environmental issues [1]. Multiples of the research on plastic polymers have been carried out, some of which are highlighted in this section. In late 2019, the outbreak of the COVID-19 pandemic resulted in a surge in the use of using single-use personal protective equipment (PPE), in particular surgical masks [2,3]. Consequently, there is increasing concern about the manner in which these masks are to be disposed of since they are disposed of in improper ways, a factor that will lead to environmental degradation. Surgical masks are usually crafted in the form of non-woven polypropylene, and their property may come in handy during waste sorting and management. [4,5]. Numerous works were devoted to measuring the effectiveness of various ways of using surgical masks in an environmentally friendly way. Such practices involved burning, landfill dumping, as well as sterilization before disposal in an effort to reduce the possible risks [6]. Other scholars investigated the possibility of recycling surgical masks to extract useful resources from them, e.g., polypropylene. The building materials and textiles, among other items, were made using the materials of masks. The research into the ways of reclaiming and reusing those materials may help to save resources and lower the volume of waste [7,8]. Researchers investigated the biodegradability of surgical mask materials in light of the trend toward more sustainable waste management practices. Some studies have assessed the potential for incorporating surgical mask components into composting processes, considering their biodegradable properties under specific conditions. Few studies investigated the potential of developing biodegradable surgical masks using sustainable materials. These masks could help alleviate the environmental impact associated with traditional single-use masks [9,10]. Other new avenues that have been researched are novel technologies of transforming used surgical masks into energy or other useful products via things such as pyrolysis or gasification. The polypropylene has a high percentage of energy content which in turn could be utilized by controlled incineration which may serve as an extra energy source to the waste-to-energy facility [11,12]. Although surgical masks are traditionally used in health care facilities to prevent infections, uses in waste management are also discussed in the context of sustainability as a whole. Whiteboards, writing boards, chalkboards or marker boards are typical learning tools that are used in brainstorming, presentations and creativity. The choice of the right writing board material is important so that it needs to be long-lasting and functional. Writing boards WBs are available in different materials so that each has different characteristics. Melamine boards: This type is composed of a paper surface infused with resin on a fiberboard and consists of a core; the boards are cheap yet tend to be stained and ghosted; the durability of the boards is decent and good enough to use in mild and moderate activities [13,14]. Porcelain steel boards or ceramic steel boards are created by gluing porcelain enamel on a metal surface, making it highly strong, hard, and removable. And, they do not get scratched or soiled, and can be used in heavy-duty and strenuous environments like schools [15,16]. Toughened safety glass in the form of tempered glass boards has a smooth appearance, excellent erasability, and great durability, albeit being likely to break when hit [17]. Acrylic boards are lightweight and a low-cost alternative that has proper erasability and average durability, but can be easily scratched and stained. The mechanical properties of these materials play a significant role in their performance. Hardness influences scratch resistance, with porcelain and glass being highly resistant, while melamine and acrylic are more vulnerable. Durability is best in porcelain and glass due to their robust nature, with melamine and acrylic being less so. Erasability is better in porcelain and glass; however, melamine and acrylic boards can stain and ghost. Impact resistance varies, with glass being the weakest and porcelain and melamine being the strongest [13-16]. An NP-complete problem is the modeling of plastic boards employing waste surgical masks as the key concern for minimizing plastic waste as part of solid waste power consumption [18].

The transmission of thermal energy is also associated with the other dimension of the research on nanofluids. Ahmed et al. [19] examined the dynamics and behaviour of gyrotactic microorganisms in magnetohydrodynamic (MHD) Eyring-Powell nanofluid flow with a focus on the influences of thermal radiation and Darcy-Forchheimer relation. The study will add to the knowledge of bioconvection in the behavior of fluids in different applications. Faizan Ahmed et al. [20] indicated the importance of the flow of bioconvection in tangent hyperbolic nanofluids, especially on the minimisation of entropy. The study is critical in the use of this in biomedical engineering and thermal management systems. Faizan Ahmed et al. [21] highlight the importance of the bioconvection flow in the tangent hyperbolic nanofluids, especially in the entropy minimization. The study is critical in the use of this in biomedical engineering and thermal management systems. Ali et al. [22] investigate the role of bioconvective studies in tangent hyperbolic nanoliquids and highlight the possibilities of improving energy systems with the mentioned property. The study is critical in explaining how nanofluids may enhance the thermal management of different processes. In bioconvection on a stretching sheet, Puneeth et al. study the thermal properties of Ree–Eyring nanofluid [23]. The study is notable because it is based on prior literature on non-Newtonian fluids and bioconvection, offering information on the heat transfer. Ali and Zaib [24] analyse the erratic flow of Eyring-Powell nanofluid near a stagnation point following a stretched sheet that has gone through convective heating. This study plays an important role in determining how the non-dynamism of nanofluids is in thermal use [24]. Ali

and Summayya [25] investigate numerical simulation of the Cattaneo -Christov theory of double-diffusion in MHD Eyring-Powell nanofluid with the emphasis on the effects of thermal radiation at a stagnation point. This research is significant in understanding fluid dynamics under complex thermal and magnetic influences.

Back propagation neural network (BP) is a form of artificial neural network that can, however, without any knowledge of the relationship between the input and the output data, simulate any non-linear or linear functional link [18, 26]. Nonetheless, BP has many drawbacks, such as long time calculation, slow convergence, and the risk of local minima. As a result, a range of hybrid optimization approaches based on global optimization algorithms were developed to increase the generalization ability of artificial neural networks [27,28]. However, because PSO is limited in its search power, it may become imprisoned in the local optima of the objective function when used to pick ANN parameters [29-31].

In 2004, a new variant of particle swarm optimization under the name quantum-behaved particle swarm optimization method was proposed [32]. Furthermore, simulation results of a variety of complicated benchmark functions revealed that QPSO outperforms the standard PSO in terms of global searching capabilities [33,34]. As a result, QPSOs are commonly utilized to tackle difficult optimization issues such as hydrothermal scheduling and economic dispatch [35,36]. However, there have been a few reports regarding employing QPSO for artificial neural network parameter calibration. To enhance the capacity for generalization and computational effectiveness of artificial neural networks, this study develops a hybrid approach for daily reservoir runoff forecasting. The QPSO algorithm is selected as the neural network's training algorithm to improve the accuracy of hydrologic forecasts. The use of Gaussian and differential sequences in GQPSO and DQPSO improves premature convergence to local optima observed in QPSO performance. However, the objective of this paper is to find out the optimum, efficient, and accurate estimate of manufacturing plastic board parameters such that two different benchmark functions, namely Elongation at fracture (EF) and Percentage of total elongation at maximum force (MF) are minimized. For this purpose, we have used an artificial neural network (ANN) based linear equation that was optimized by using Particle swarm optimization and its different improved versions of PSO. Briefly, the contributions of this research are as follows:

- Implement the linear model using an artificial neural network with input-output parameters of the plastic board using a waste surgical mask.
- To optimize material composition using ANN via comprehensive fractional design based on process modeling.
- Using PSO and its three upgraded PSO approaches, the impacts of the input variables (polypropylene (PP), Maleic anhydrite Grafted polypropylene (MA), Titanium dioxide (TiO2), and Tensile Strength (TS)) on two responses (Elongation at fracture (EF) and Percentage of total elongation at maximum force (MF)) were explored and optimized.

The remainder of the paper is organized as follows: Section 2 discusses the materials and techniques of the current study, followed by Section 3, which describes Neural network modeling and characteristics of various advanced PSO for continuous optimization. Section 4 discusses nonlinear model optimization strategies. Section 5 presents the results of the optimization and compares the methods of solving case studies of engineering troubles. Lastly, Section 6 will provide a conclusion to the paper.

MATERIALS AND METHOD

Initially, discarded surgical masks undergo a cleaning process and are subsequently shredded into small fibrous components. The masks, PP, and TiO2 are then blended using various mixing ratios utilizing a Sigma blade mixer from Brabender, Germany. This blending operation lasts 5 minutes at a temperature of 180°C, with MA-g-PP acting as the compatibilizer. Subsequently, the composite material undergoes compression molding at a temperature of 160°C and is maintained for 5 minutes to achieve the intended thickness. Finally, tensile testing samples are taken from the molded sheet having a 30mm gauge length, 4.31mm width, and a thickness of 1.85mm (approx.). Tensile tests are carried out with a tensile testing instrumentfollowing ASTM D638and three specimens for each different composition. Throughout all scenarios, the strain rate is kept constant at 50mm/min. Figure 1 depicts the experimental approach of the current study, whereas Figures 2 and 3 depict the results of the process. Table 1 shows the input parameters and their ranges.

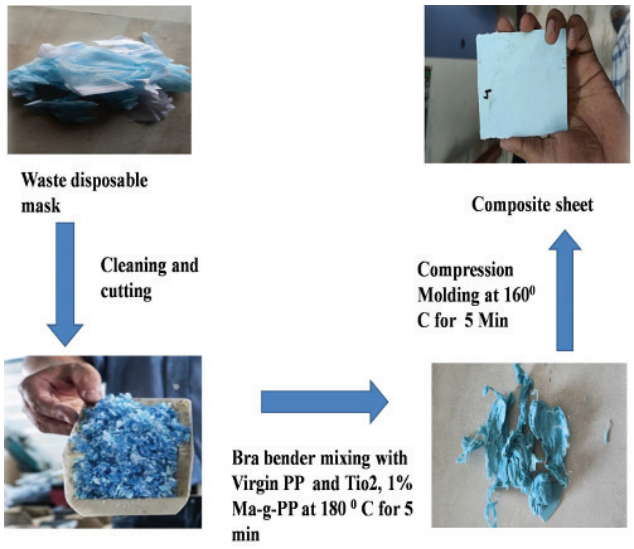

Figure 1. The methodology used in the present research.

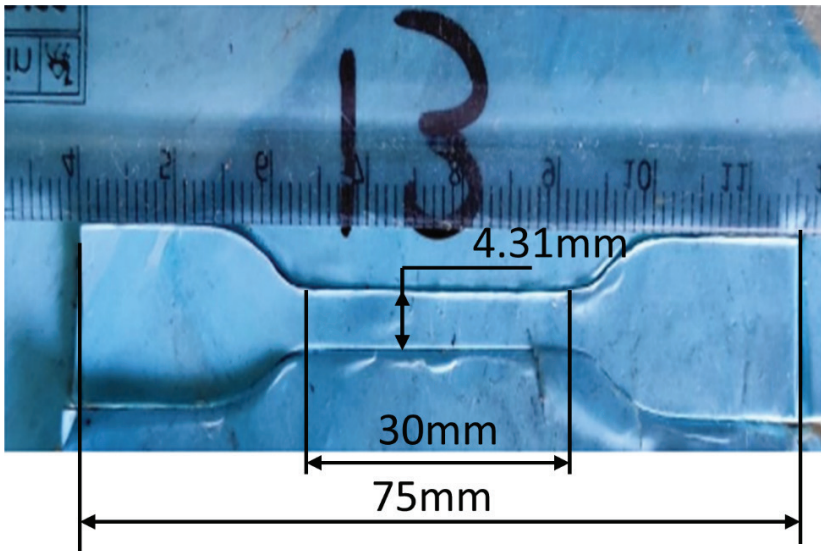

Figure 2. Tensile testing sample made of the composite.

(a)

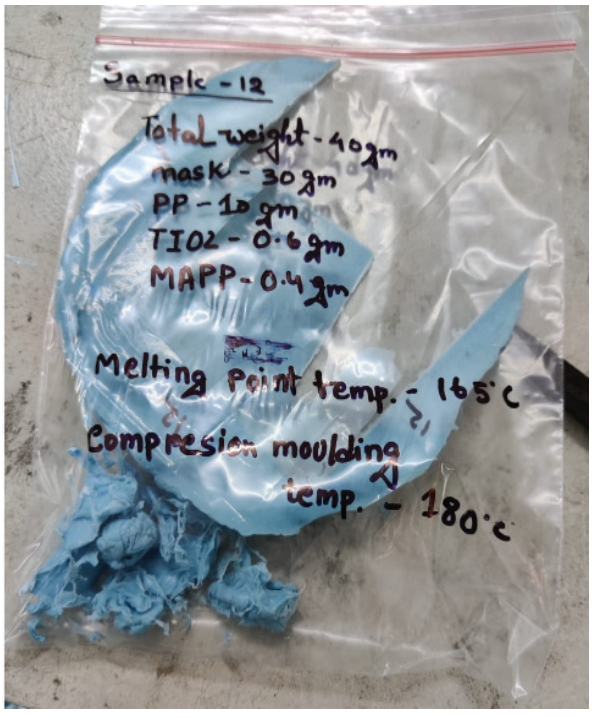

(b)

Figure 3. (a) Sigma blade mixer &(b) plastic board.

Table 1. Range of input parameters

Process Parameters (Variables)	Range	
	LB	UB
PP (%)	10	30
MA (%)	3	28
TiO_2 (%)	0	0.6
TS (%)	10.229	27.98

MATHEMATICAL MODELLING

Neural Network Model for Elongation at Fracture (EF) and Percentage of Total Elongation at Maximum Force (MF)

From the experimental work, it has been observed that there is a certain linear relationship between process input variables, Polypropylene (PP), Maleic anhydride Grafted Polypropylene (MA), Titanium dioxide (TI), and Tensile Strength (TS), with output variables Elongation at Fracture

(EF) and Percentage of Total Elongation at Maximum Force (MF). Now, the fitness function (FF) of improved versions of PSO for this work is the obtained regression equation of Elongation at Fracture (EF), and Maximum Force (MF), which is a function of Polypropylene (PP), Maleic anhydride Grafted Polypropylene (MA), Titanium dioxide (TiO2), and Tensile Strength (TS). A simple Neuron with no buried layers represents a linear function. As a consequence, it is possible to write it as

$$FF = EF = f_1 (PP, MA, TI, TS) \quad (1)$$

$$FF = MF = f_2 (PP, MA, TI, TS) \quad (2)$$

The objective is to determine the best condition (optimal values of PP, MA, TiO2, and TS) to minimize the value of EF and MF. During the mathematical formulation of the ANN model using input and output variables, Polypropylene (PP), metal removal rate (MA), Titanium oxide (TiO2), and TS are kept in input nodes, whereas Elongation at fracture (EF) and Percentage of total elongation at maximum force (MF) are output layer nodes of the ANN model. Therefore, the dimension of the search for an improved version of PSO is 5. The weights w_1,w_2, w_3, w_4 re-applied to the three inputs, while the bias term β is assigned to the output node. The absence of an activation function is not a classification issue in this circumstance. As a consequence, using a neural network model, Elongation at fracture (EF) and Percentage of total elongation at maximum force may be stated as follows

$$EF = PP * w_{1,E} + MA * w_{2E} + TI * w_{3,E} + TS * w_{4,E} + \beta_E \quad (3)$$

$$MF = PP * w_{1,M} + MA * w_{2,M} + TI * w_{3,M} + TS * w_{4,M} + \beta_M \quad (4)$$

Now we have to determine the most optimal values for the weights and bias parameters in equations 3 and 4. We employed particle swarm optimization and its improved version to optimize the ANN model implemented for two response variables, EF and MF, respectively. The proposed NN model was created using training datasets gathered through experiments. Proposed algorithms are used to find the coefficient of w_1,w_2, w_3, w and β So that squared error should be minimum [37-39].

$$E = \sum_{i=1}^{m} (t_i - c_i)^2 \quad (5)$$

Where t and c are the targets and estimated outputs from the training data, and E is the objective function.

Quantum Particle Swarm Optimization (QPSO) Evolutionary Strategy in Process Modelling

In classical mechanics, a particle is represented by its location vector x_i and velocity vector v_i, which defines the particle's journey. In Newtonian mechanics, the particle proceeds following a predetermined course, but this is not the case in quantum mechanics. The word trajectory has no significance in the quantum realm since x_i and v_i, of a particle, following the uncertainty, exhibits quantum behavior, the PSO algorithm is bound to behave differently [26]. Instead of position and velocity, the state of a particle is expressed by wave function ψ(x, t) (Schrödinger equation) [27] in the quantum form of a PSO termed QPSO. The probability of the particle occurring in location xi from the probability density function $\|\psi(x,t)\|^2$ [28]. When applying the Monte Carlo technique, the particles move in accordance with the iterative equation [28-30]. Its position $x_i(t + 1)$ may now be computed using the following equation:

$$\begin{aligned} x_i(t+1) &= p + \beta \, \|Mbest_i - x_i(t)\| . \ln\left(\frac{1}{u}\right) \text{ if } k \geq 0.5 \\ x_i(t+1) &= p - \beta \, \|Mbest_i - x_i(t)\| . \ln\left(\frac{1}{u}\right) \text{ if } k < 0.5 \end{aligned} \quad (6)$$

where b is a contraction-expansion coefficient, u is a design parameter, and k [38] are values created using uniform probability distribution functions in the range [0, 1]. Mean Best (M_{best}) The population's global point is defined as the mean of P_{best} locations of all particles

$$Mbest_i = \frac{1}{N} \sum_{i=1}^{N} p_{gd}(t) \quad (7)$$

The best particle index by "g" among all the particles and a local attractor of PSO convergence has the following coordinates:

$$p = \frac{(c_1 p_{id} + c_1 p_{gd})}{c_1 + c_2} \quad (8)$$

Quantum-Behaved Particle Swarm Optimization Using Gaussian Mutation (GQPSO)

Uniform probability distribution is a method that most commonly produces random numbers. However, another new technique can be used to update the PSO velocity by the use of Gaussian, Cauchy, and exponential probability distributions [35]. In GQPSO, we offer a mutation operator in QPSO using a Gaussian probability distribution. For the stochastic coefficients of GQPSO, generating Gaussian distribution sequences with zero mean and unit variance abs [N(0,1)] may provide a good compromise to move away from the current point and escape from local minima (Table 2). These novel QPSO techniques in conjunction with the mutation operator are as follows:

Approach 1: Update the positional vector with the following equation:

$$\begin{aligned} x_i(t+1) &= p + \beta \, \|Mbest_i - x_i(t)\| . \ln\left(\frac{1}{G}\right) \text{ if } k \geq 0.5 \\ x_i(t+1) &= p - \beta \, \|Mbest_i - x_i(t)\| . \ln\left(\frac{1}{G}\right) \text{ if } k < 0.5 \end{aligned} \quad (9)$$

where G = abs (N(0,1)).

Approach 2: Update the parameters c_1 and c_2 by the following equation:

$$p = \frac{(G.p_{id}+g.p_{gd})}{c_1+c_2} \quad (10)$$

Where, g =abs [N(0,1)]. Approach 3: This approach uses Eqn. (9) and (10)

OPTIMIZATION OF MATHEMATICAL MODEL

Table 3 represents the basic parameters of PSO and quantum-inspired PSO. In this section, three linear NN model response variable equations (Eqn. 11- Eqn. 18) optimized by PSO, QPSO, DQPSO, and GQPSO& finally obtained the co-efficient (shown in Table 3) & their response variable equations respectively. To execute this algorithm, we used MATLAB 2013A with processor specification 11th Gen Intel(R) Core (TM) i5-1155G7 @ 2.50GHz 2.50 GHz. As the algorithms are heuristics so there is a chance that in every iteration it produces a different fitness value, for this reason, we run each algorithm 10 times with several iterations taken 1000, 2000, 3000,4000 & 5000 respectively, and all values are taken as average from the outcomes.

Model Validation on Testing Dataset

Table 5 & Table 6 represent the average computational time for all the algorithms during cross-validation & RMSE. Where, accuracy in % = (100-RMSE) in %.

Response variable equation obtained after the optimization of NN model representing by the following equations:

$$(EF)_{DQPSO\text{-}ANN} = -0.3792*PP - 0.3391*M + 7.0282*TI - 0.0381*TS + 15 \quad (13)$$

$$(EF)_{GQPSO\text{-}ANN} = -0.42166*PP - 0.4109*M + 15*TI - 0.02200*TS + 12.832 \quad (14)$$

Table 2. Flow chart of the proposed ANN-GQPSO-based method

Preparation	Step 1	Set the GQPSO to maximize iterations and population size
		Divide the total data into training and validation sets
		Define the transfer function of neurons
		Both the training and validation datasets are normalized
		Encode each particle by the initial connection weights vector and the thresholds vector of the ANN
Initialization	Step 2	Start the evolution from the 1st generation
		Randomize a fixed population of different individual networks (weights of all connections & initial threshold)
Evolution	Step 3	Construct a network with the corresponding particles one by one.
		Input the training & testing data into each constructed network
		Compute the values of the objective function for all networks
		Update the best-known position of each and the whole population
		Calculate the mean best position of the whole population
		Calculate the contraction-expansion coefficient
		Reproduce the subpopulation by updating the particle swarm position
Prediction	Step 4	Maximum iteration reached if yes go to Step 3
		Otherwise, increase the maximum iteration by 1 & go to the next Step
		The optimal model is obtained
		The forecast value is obtained
		Stop

Table 3. Parameters of PSO and QPSO

Parameters of PSO	Parameters of QPSO
Inertia Weight, w=1	Inertia weight, w_1 = 0.5; w_2 = 1.0;
Inertia Weight Damping Ratio, W_{damp} =0.99	Personal Learning Coefficient, c_1 = 1.5; c_2 = 1.5;
Personal Learning Coefficient, c_1=1.5;	No. of Populations: n_{pop}=100
Global Learning Coefficient, c_2 =2.0;	
No. of Populations: n_{pop}=100	

Table 4. Coefficient of NN model of response variable

Name of the algorithms	Coefficients of the NN model after Elongation at Fabrication (EF) Optimizations				
	w_1	w_2	w_3	w_4	$ß$
PSO	0.02781	0.00458	1.0148	0.1830	-1.5222
QPSO	0.359707	0.2848	-3.882	0.3584	-15
DQPSO	-0.3792	-0.3391	7.0282	-0.0381	15
GQPSO	-0.42166	-0.4109	15	-0.02200	12.832
Name of the algorithms	**NN model coefficients after optimization of Percentage of total elongation at maximum force (MF)**				
	w_1	w_2	w_3	w_4	$ß$
PSO	-0.0069	-0.0109	0.4213	0.0411	0.3216
QPSO	-1.1755	-1.5437	0.2425	-1.1315	3.1451
DQPSO	-0.3685	-0.3163	5.7625	-0.1528	15
GQPSO	0.37045	0.3077	-5.1539	0.2437	-15

Table 5. Time required to compute both objective functions maximum force elongation facture and percentage of total elongation

Name of algorithm	Computation time in Sec.	
	Elongation at Facture (EF)	Elongation at maximum Force (MF)
PSO	70.535	108.412
QPSO	25.48	29.76530.25
DQPSO	64.77	30.826
GQPSO	32.76	24.952

Table 6. Model accuracy of testing dataset

Name of algorithm	RMSE in %	
	Elongation at facture (EF)	Elongation at maximum force (MF)
PSO	4.35826	5.89261
QPSO	3.05068	4.66867
DQPSO	2.74599	4.62517
GQPSO	2.37064	2.58097

$$(MF)_{PSO\text{-}ANN} = -0.0069*PP - 0.0109*M + 0.4213*TI + 0.0411*TS + 0.3216 \quad (15)$$

$$(MF)_{QPSO\text{-}ANN} = -1.1755*PP - 1.5437*MA + 0.2425*TI - 1.1315*TS + 3.1451 \quad (16)$$

$$(MF)_{DQPSO\text{-}ANN} = -0.3865*PP - 0.3163*M + 5.7625*TI - 0.1528*TS + 15 \quad (17)$$

$$(MF)_{GQPSO\text{-}ANN} = 0.3705*PP + 0.3077*MA - 5.1539*TI + 0.2437*TS - 15 \quad (18)$$

Figure 4 and Figure 5 shows the deviation characteristics of PSO-ANN, QPSO-ANN, DQPSO-ANN & GQPSO-ANN algorithms for both the response variables Elongation at fracture (EF) and Percentage of total elongation at maximum force (MF). Figure 6 represents the objective function of all the algorithms during model validation.

RESULT AND DISCUSSION

All the techniques are simulated using MATLAB 2015a in a computer with 16 GB RAM, Processor11th Gen Intel(R) Core (TM) i5-1155G7 @ 2.50GHz, 2496 Mhz, 4 Core(s), 8 Logical Processor(s) and Windows11 Operating System.

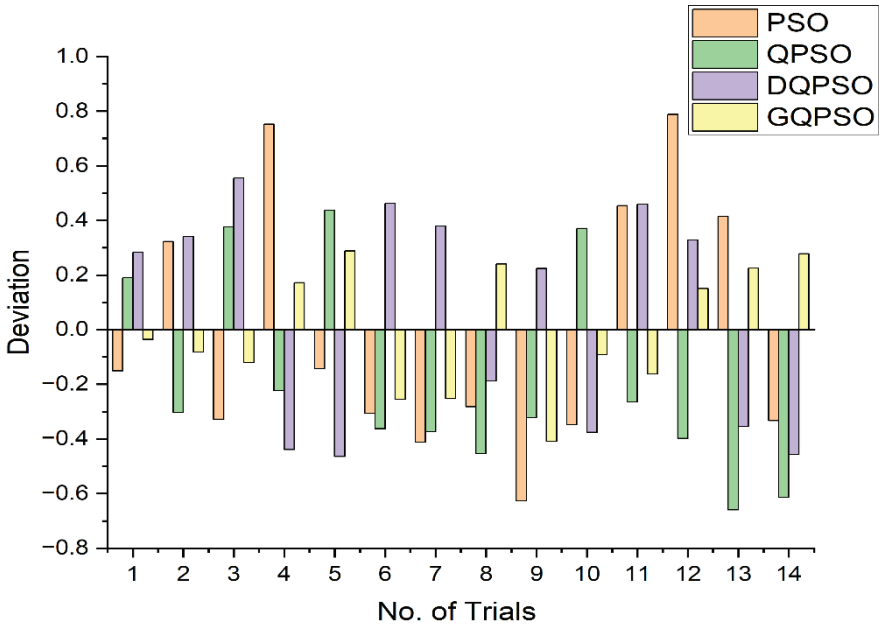

Figure 4. A comparative study based on Elongation at fracture (EF).

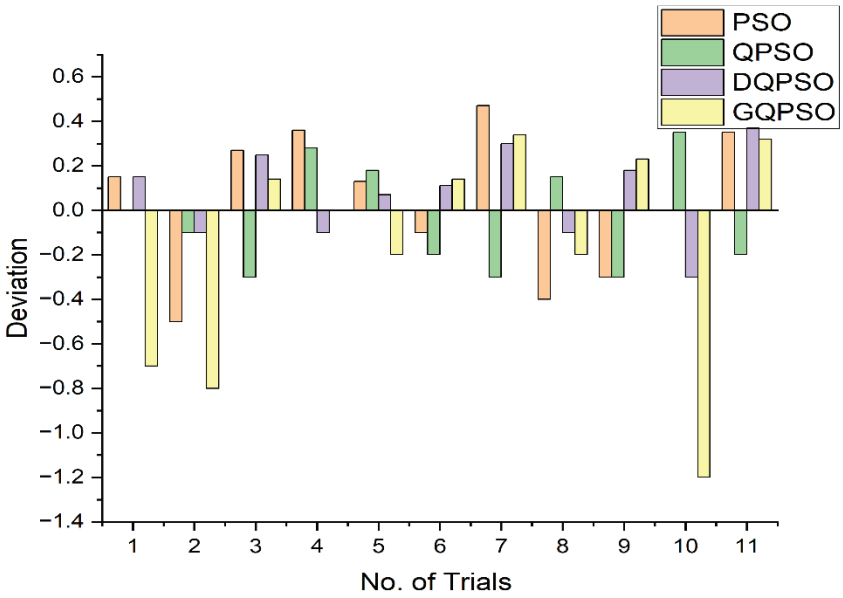

Figure 5. Comparative study based on and percentage of total elongation at maximum force (MF).

Cross-validation of Model

This part compares four computational models, PSO-ANN, QPSO-ANN, DQPSO-ANN, and GQPSO-ANN to determine the best-fitting model based on 16 experimental datasets. To do this, each set of input variables is entered into Eqn. 11-14 to determine the response variables of Elongation at fracture (EF) and Percentage of total elongation at maximum force (MF). The cross-validation comparison research for EF and MF is given in Figures 1 and 2. Table 6 depiction clearly shows that the GQPSO-ANN model outperformed other upgraded PSO-ANN models. Another significant aspect of determining the optimum optimization model is computational time.

Model Prediction Based on Improved PSO-ANN

Model validation is done in this portion for 10% of the experimental dataset (2 experimental data). Table 5 compares model validation between PSO-ANN and three

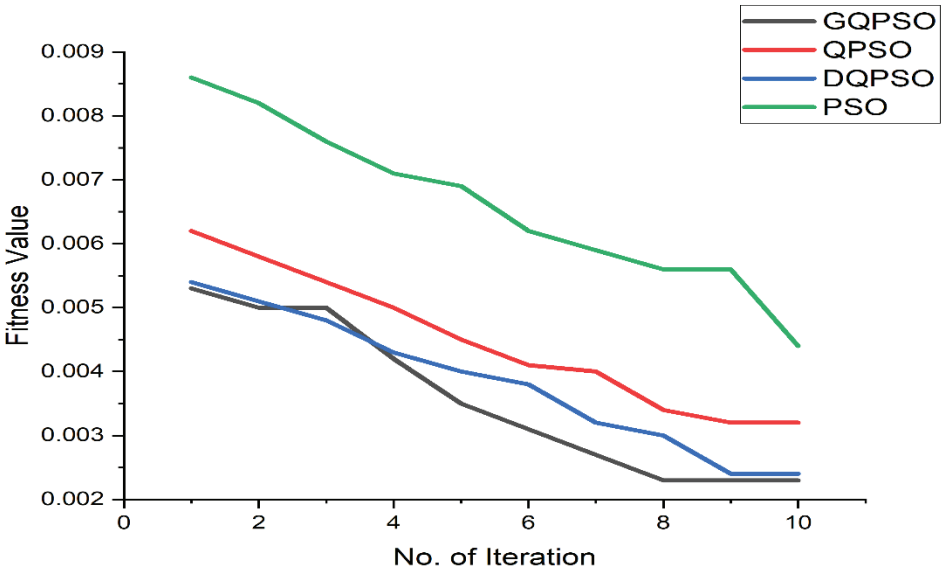

Figure 6. A comparative study based on Fitness value.

Table 7. Model accuracy of cross-validation dataset

s	RMSE in %	
	Elongation at facture (EF)	**Elongation at maximum force (MF)**
PSO	8.562	7.2916
QPSO	6.8605	7.7686
DQPSO	5.9747	4.7612
GQPSO	4.4670	3.9708

upgraded PSO-ANN procedures (QPSO-ANN, DQPSO-ANN, and GQPSO-ANN). According to the results, the average RMSE for GQPSO-ANN in response variables EF& MF is much lower.

Optimal Condition for ANN Based Model

According to the preceding section, GQPSO-based ANN beat the other three optimization models in cross-validation and model prediction. In this phase, the best conditions for proper modeling of manufactured plastic boards are determined by searching for optimal values of polypropylene (PP), Maleic anhydrite grafted polypropylene (MA), Titanium dioxide (TiO_2), and tensile strength (TS), such that elongation at fracture (EF) and percentage of total elongation at maximum force (MF) ismaximized. A new fitness function (OF) is defined as a combination of EF and MF by their numerical values.

$$OF = (EF)_{GQPSO\text{-}ANN} + (MF)_{GQPSO\text{-}ANN}$$

$$\begin{aligned} OF = {} & (-0.0069*PP - 0.0109*MA + 0.4213*TI \\ & + 0.0411*TS + 0.3216) + (0.3705*PP \\ & + 0.3077*MA - 5.1539*TI + 0.2437*TS - 15) \end{aligned} \quad (19)$$

Maximum polypropylene (PP) concentration is 29.678%, minimum Maleic anhydrite Grafted polypropylene (MA) concentration is 11.082%, maximum Titanium dioxide (TiO2) concentration is 0.4412%, and maximum Tensile Strength (TS) is 26.712. GQPSO is the best evolutionary algorithm to minimize the combined objective function (OF) of the developed neural models for EF and MF. OF will have the highest value when PP, TiO2, and TS have the highest values and MA has the lowest value. This determined optimal value has been confirmed by experimental data, indicating that the output of this procedure is extremely excellent. The GQPSO-NN model takes 23.931 seconds to achieve the optimal condition.

CONCLUSION

The parametric analysis of plastic boards employing waste surgical maskswas performed in our current study. The efficient and accurate estimate of manufacturing plastic board characteristics depends on two potential functions, Elongation at fracture (EF) and Percentage of total elongation at maximum force (MF). To achieve the optimal

estimate of plastic board characteristics we performed three improved particle swarm optimization techniques. The outcomes of the present research are drawnout below:

1. Elongation at fracture (EF) and Percentage of total elongation at maximum force (MF) increased by increasing the concentration of independent variables such as material compositions of material composition of polypropylene (PP), Titanium dioxide (TiO2), and Tensile Strength (TS), while keeping Maleic anhydrite Grafted Polypropylenes (MA) as minimum value.
2. Overall dataset split into 9:1 ratio for perform cross-validation and model validation. During cross-validation, it has been observed that proposed all ANN-based improved PSO techniques obtained better accuracy but ANN-based GQPSO achieved the maximum accuracy in both the response variables Elongation at fracture (EF) and Maximum force (MF) about 95.533% and 96.0292% respectively.
3. For multi-response optimization, the optimal parametric conditions for polypropylene (PP), Maleic anhydrite Grafted polypropylene (MA), Titanium dioxide (TiO2), and Tensile Strength (TS) during waste surgical mask design are 29.678%, 11.082%, 0.4412%, and 26.712, respectively.
4. The Gaussian Quantum behaved Particle Swam Optimization (GQPSO)-based artificial neural network (ANN) optimization technique is more suitable than artificial neural network (ANN) optimized Particle Swam Optimization (PSO), Quantum behaved Particle Swam Optimization (QPSO), and Differential Quantum behaved Particle Swam Optimization (DQPSO) using computation time, better cross-validation, and best-fitted model for testing dataset.
5. The model's accuracy may be increased further by increasing the number of experimental datasets and employing various mathematical models (Response Surface Methodology & Analysis of variance) optimized heuristic optimization approaches.

AUTHORSHIP CONTRIBUTIONS

Authors equally contributed to this work.

DATA AVAILABILITY STATEMENT

The authors confirm that the data that supports the findings of this study are available within the article. Raw data that support the finding of this study are available from the corresponding author, upon reasonable request.

CONFLICT OF INTEREST

The author declared no potential conflicts of interest with respect to the research, authorship, and/or publication of this article.

ETHICS

There are no ethical issues with the publication of this manuscript.

STATEMENT ON THE USE OF ARTIFICIAL INTELLIGENCE

Artificial intelligence was not used in the preparation of the article.

REFERENCES

[1] Derman S, Kızılbey K, Akdeste ZM. Polymeric nanoparticles. Sigma J Eng Nat Sci 2013;31:107–120.

[2] Şahin Fİ, Acaralı N. Evaluation of properties for synthetic polymers in medicine. Sigma J Eng Nat Sci 2014;42:1315–1324.

[3] Aragaw TA. Surgical face masks as a potential source for microplastic pollution in the COVID-19 scenario. Mar Pollut Bull 2020;159:111517. [CrossRef]

[4] Rowan NJ, Laffey JG. Unlocking the surge in demand for personal and protective equipment (PPE) and improvised face coverings arising from coronavirus disease (COVID-19) pandemic: Implications for efficacy, re-use and sustainable waste management. Sci Total Environ 2021;752:142259. [CrossRef]

[5] Mondal R, Mishra RS, Pillai JK, Sahoo M. COVID-19 pandemic and biomedical waste management practices in healthcare system. J Fam Med Prim Care 2022;11:439. [CrossRef]

[6] Selvaranjan K, Navaratnam S, Rajeev P, Navintherakumaran N. Environmental challenges induced by extensive use of face masks during COVID-19: A review and potential solutions. Environ Chall 2021;3:100039. [CrossRef]

[7] Maderuelo-Sanz R, Acedo-Fuentes P, García-Cobos FJ, Sánchez-Delgado FJ, Mota-López I, Meneses-Rodríguez JM. The recycling of surgical face masks as sound porous absorbers: Preliminary evaluation. 2021;786:147461. [CrossRef]

[8] Occasi G, De Angelis D, Scarsella M, Tammaro M, Tuccinardi L, Tuffi R. Recovery material from a new designed surgical face mask: A complementary approach based on mechanical and thermo-chemical recycling. J Environ Manag 2022;324:116341. [CrossRef]

[9] Ray SS, Lee HK, Huyen DTT, Chen SS, Kwon YN. Microplastics waste in environment: A perspective on recycling issues from PPE kits and face masks during the COVID-19 pandemic. Environ Technol Innov 2022;26:102290. [CrossRef]

[10] Hasija V, Patial S, Kumar A, Singh P, Ahamad T, Khan AAP, et al. Environmental impact of COVID-19 vaccine waste: A perspective on potential role of natural and biodegradable materials. J Environ Chem Eng 2022;10:107894. [CrossRef]

[11] Dharmaraj S, Ashokkumar V, Chew KW, Chia SR, Show PL, Ngamcharussrivichai C. Novel strategy in biohydrogen energy production from COVID-19 plastic waste: A critical review. Int J Hydrogen Energy 2022;47:42051–42074. [CrossRef]

[12] Yousef S, Eimontas J, Zakarauskas K, Jančauskas A, Striūgas N. An eco-friendly strategy for recovery of H2-CH4-rich syngas, benzene-rich tar, and carbon nanoparticles from surgical mask waste using an updraft gasifier system. 2023;45:5063–5080. [CrossRef]

[13] Mili M, Hashmi SAR, Ather M, Hada V, Markandeya N, Kamble S, et al. Novel lignin as natural-biodegradable binder for various sectors—A review. J Appl Polym Sci 2022;139:51951. [CrossRef]

[14] Mullins MJ, Liu D, Sue HJ. Mechanical properties of thermosets. In: Thermosets: Structure, Properties, and Applications. 2nd ed. Amsterdam: Elsevier; 2018. p. 35–68. [CrossRef]

[15] Franzoni E, Pigino B, Graziani G, Lucchese C, Fregni A. A new prefabricated external thermal insulation composite board with ceramic finishing for buildings retrofitting. Mater Struct 2016;49:1527–1542. [CrossRef]

[16] Spector M, Johnson C. Porcelain coated steel printed wiring boards. In: 1979 EIC 14th Electrical/Electronics Insulation Conference. 1979;339–343. [CrossRef]

[17] Stull AT, Fiorella L, Gainer MJ, Mayer RE. Using transparent whiteboards to boost learning from online STEM lectures. Comput Educ 2018;120:146–159. [CrossRef]

[18] Pekel E, Kara SS. A comprehensive review for artificial neural network application to public transportation. Sigma J Eng Nat Sci 2017;35:157–179.

[19] Ahmed MF, Zaib A, Ali F, Bafakeeh OT, Tag-ElDin ESM, Guedri K, et al. Numerical computation for gyrotactic microorganisms in MHD radiative Eyring–Powell nanomaterial flow by a static/moving wedge with Darcy–Forchheimer relation. Micromachines 2022;13:1768. [CrossRef]

[20] Ahmed FM, Khalid M, Ali F, Al-Bossly A, Alduais FS, Eldin SM, Saeed A. Importance of bioconvection flow on tangent hyperbolic nanofluid with entropy minimization. Front Phys 2023;11:1154478. [CrossRef]

[21] Ali F, Loganathan K, Eswaramoorthi S, Faizan M, Prabu E, Zaib A. Bioconvective applications of unsteady slip flow over a tangent hyperbolic nanoliquid with surface heating: Improving energy system performance. Int J Appl Comput Math 2022;8:276. [CrossRef]

[22] Ali F, Padmavathi T, Hemalatha B. Entropy minimization in darcy forchheimer on sutterby nanofluid past a stretching surface with swimming of gyrotactic microorganisms. Waves Rand Complex Media 2022;35:10333–10356. [CrossRef]

[23] Puneeth V, Ali F, Khan MR, Anwar MS, Ahammad NA. Theoretical analysis of the thermal characteristics of Ree–Eyring nanofluid flowing past a stretching sheet due to bioconvection. Biomass Convers Biorefinery 2024;14:8649–8660. [CrossRef]

[24] Ali F, Zaib A. Unsteady flow of an Eyring-Powell nanofluid near stagnation point past a convectively heated stretching sheet. Arab J Basic Appl Sci 2019;26:215–224. [CrossRef]

[25] Ali F, Summayya N. Numerical simulation of Cattaneo–Christov double-diffusion theory with thermal radiation on MHD Eyring–Powell nanofluid towards a stagnation point. Int J Ambient Energy 2022;43:4939–4949. [CrossRef]

[26] Demir S. Artificial neural network simulation of advanced biological wastewater treatment plant performance. Sigma J Eng Nat Sci 2020;38:1713–1728.

[27] Chau KW. Particle swarm optimization training algorithm for ANNs in stage prediction of Shing Mun River. J Hydrol 2006;329:363–367. [CrossRef]

[28] Asadnia M, Chua LHC, Qin XS, Talei A. Improved particle swarm optimization based artificial neural network for rainfall-runoff modeling. J Hydrol Eng 2014;19:1320–1329. [CrossRef]

[29] Liu WC, Chung CE. Enhancing the predicting accuracy of the water stage using a physical-based model and an artificial neural network-genetic algorithm in a river system. Water 2014;6:1642–1661. [CrossRef]

[30] Dutta P, Cengiz K, Kumar A. Study of bio-inspired neural networks for the prediction of liquid flow in a process control system. In: Cognitive Big Data Intelligence with a Metaheuristic Approach. New York: Academic Press; 2022. p. 173–191. [CrossRef]

[31] Jeong DI, Kim YO. Combining single-value streamflow forecasts—A review and guidelines for selecting techniques. J Hydrol 2009;377:284–299. [CrossRef]

[32] Sun J, Feng B, Xu WB. Particle swarm optimization with particles having quantum behavior. In: Proceedings of the 2004 Congress on Evolutionary Computation, CEC2004. Portland, OR, USA; 2004. p. 325–331.

[33] Fang W, Sun J, Ding Y, Wu X, Xu W. A review of quantum-behaved particle swarm optimization. IETE Tech Rev 2010;27:336–348. [CrossRef]

[34] Xi M, Sun J, Xu W. An improved quantum-behaved particle swarm optimization algorithm with weighted mean best position. Appl Math Comput 2008;205:751–759. [CrossRef]

[35] Mondal K, Mallick B, Hameed AS, Sarkar A, Mahato J, Dutta P. Experimental analysis and hybrid-optimization of micro-ECDM process parameters to enhance micro-machining performances of silica by Gaussian-Quantum-PSO. J Adv Manuf Syst 2024;241:125–141. [CrossRef]

[36] Sun C, Lu S. Short-term combined economic emission hydrothermal scheduling using improved quantum-behaved particle swarm optimization. Expert Syst Appl 2010;37:4232–4241. [CrossRef]

[37] Dutta P, Kumar A. Design an intelligent calibration technique using optimized GA-ANN for liquid flow control system. J Eur Syst Autom 2017;50:449. [CrossRef]

[38] Dutta P, Kumar A. Modeling and optimization of a liquid flow process using an artificial neural network-based flower pollination algorithm. J Intell Syst 2018;29:787–798. [CrossRef]

[39] Bellubbi S, Mallick B, Hameed AS, Dutta P, Sarkar MK, Nanjundaswamy S. Neural network (NN)-based RSM-PSO multiresponse parametric optimization of the electro chemical discharge micromachining process during microchannel cutting on silica glass. J Adv Manuf Syst 2022;21:869–897. [CrossRef]